This term is negligible in the more commonly observed dilute case such as described by Swift and Connick[30] in which the paramagnetic shift reagent is present in much lower concentration than the diamagnetic substrate.

Registry No. IIIa, 64612-05-1; IIIb, 78685-54-8; IIIc, 78685-55-9; IIId, 78685-56-0; IIIe, 78685-57-1; IIIf, 78685-58-2; IIIg, 78685-59-3; IIIh, 78685-60-6; IIIi, 78685-61-7; IIIj, 78685-62-8; IIIk, 78685-63-9; $Eu(fod)_3$, 17631-68-4; [4,4′-(ethylenedinitrilo)di-2-pentanonato(2−)]cobalt, 36802-26-3; [3,3′-(ethylenedinitrilo)di-3-hexanonato(2−)]cobalt, 78685-64-0; [2,2′-(ethylenedinitrilo)di-3-chloro-2-pentanonato(2−)]cobalt, 78685-65-1; [2,2′-(ethylenedinitrilo)di-3-bromo-2-pentanonato(2−)]cobalt, 78685-66-2; [4,4′-(ethylenedinitrilo)di-1,1,1-trifluoro-2-pentanonato(2−)]cobalt, 35816-74-1; [5,5′-(ethylenedinitrilo)di-2,2-dimethyl-3-hexanonato(2−)]cobalt, 78685-67-3; [3,3′-(ethylenedinitrilo)di-1-phenyl-1-butanonato(2−)]cobalt, 36802-28-5.

(30) Swift, T. J.; Connick, R. E. *J. Chem. Phys.* **1962**, *37*, 307–320.

Contribution from the Laboratoire d'Optique Physique (ER 5), EPCI, 10 rue Vauquelin, 75231 Paris Cedex 05, France, and the Laboratoire de Spectrochimie des Elêments de Transition (ERA 672), Université de Paris Sud, 91405 Orsay, France

Spectroscopic and Magnetic Properties of $Cs_3Ti_2Cl_9$

B. BRIAT,*[1a] O. KAHN,*[1b] I. MORGENSTERN-BADARAU,[1b] and J. C. RIVOAL[1a]

Received December 24, 1980

The title compound has been obtained as large single crystals of good optical quality. A series of experiments have been performed on it, in a wide temperature range, in order to describe properly the ground state manifold on the $Ti_2Cl_9^{3-}$ binuclear unit. These include EPR, Raman, and infrared and visible absorption spectroscopy and magnetic circular dichroism (MCD) as well as magnetic susceptibility measurements. Among our results, infrared and magnetic data have been especially fruitful since they prove unambiguously that, for each of the $TiCl_6^{3-}$ units, the trigonal field is very large, with $^2A_1$ lying about 1500 cm^{-1} below ^2E. All our other data are consistent with that interpretation. The lowest lying terms in our system are therefore $^1A_1'$ and $^3A_2''$ arising from the exchange interaction between two $^2A_1$ states. An analysis of the temperature dependence of $\chi_\parallel$ and $\chi_\perp$ indicates very clearly that $^1A_1'$ is lowest, the energy gap $^1A_1'-^3A_2''$ being roughly $J = -525$ cm^{-1}. The above values for the trigonal field Δ and for J have been obtained on the basis of a static model, which we believe is essentially correct. In view however of a slight discrepancy between our susceptibility data and the model predictions, we searched for an improvement of the theory. We show that vibronic coupling might be responsible for the observed increase of $|J|$ when T is lowered from room to liquid helium temperature. Finally, the difference in behavior between $Cs_3Ti_2Cl_9$ and $Cs_3Cr_2Cl_9$ regarding the order of magnitude of exchange interactions is briefly discussed. Our EPR results indicate that $Cs_3Ti_2Cl_9$ is a very favorable matrix to study the coupling of any paramagnetic ions added intentionally.

Introduction

A great effort is presently being made toward a better understanding of the spectroscopic and magnetic properties of clusters of transition-metal ions. These serve as molecular models for checking physical concepts and are of some relevance to spin glasses. Among those clusters, the confacial, bioctahedral anions $M_2Cl_9^{3-}$ have long been known but they are still of current interest. Recent work includes, for example, the synthesis of ions containing two different metal atoms,[2] a reinvestigation of the crystal structure of $Cs_3Sc_2Cl_9$,[3] and answers to questions related to the optical spectra of molybdenum and tungsten derivatives.[4]

Among the $A_3M_2X_9$ (X = Cl, Br) structures, those with M = Cr,[5] Ti, or V (space group D_{6h}^4-$P6_3/mmc$ with $Z = 2$) deserve particular attention since they contain discrete, isolated dinuclear units of high symmetry (D_{3h}) having their threefold axis coinciding with the c axis of the crystal. By contrast with heavily doped matrices (e.g., Al_2O_3), which contain clusters of various symmetries, such materials are therefore ideally suited to a detailed investigation of exchange interaction within isolated pairs. Indeed, during the past few years, availability of single crystals of sufficient size has quite naturally stimulated a great deal of activity in this area.

The chromium derivatives have been chosen first since they present favorable circumstances from both an experimental and a theoretical viewpoint; Cr^{3+} is well-known to show sharp lines in its optical spectrum, and it has a spin-only ground state. Published work on the $Cr_2X_9^{3-}$ anions includes an analysis of their optical and magnetooptical properties in the visible and near-UV[6,7] and magnetic[8] and EPR[9] as well as Raman[10,11] and infrared studies.[10] All these measurements lead to an unambiguous description of the ground-state manifold and to detailed information regarding several excited spectroscopic terms of the chromium pairs.

From a theoretical viewpoint, the study of titanium pairs is challenging for especially two reasons. First, difficulties arise when both orbital and spin angular momentums have to be taken into account in the treatment of exchange interactions. Models have been proposed,[12–16] but they remained largely unexploited due to the paucity of experimental data. Previous work on $Cs_3Ti_2Cl_9$ or related systems has not been performed under ideal experimental conditions. Optical spectra have been taken on solids[17,18] or solutions,[2] but their dependence upon

(1) (a) EPCI. (b) Université de Paris Sud.
(2) M. S. Matson and R. A. D. Wentworth, *Inorg. Chem.*, **15**, 2139 (1976).
(3) K. R. Poeppelmeier, J. D. Corbett, T. P. McMullen, D. R. Torgeson, and R. G. Barnes, *Inorg. Chem.*, **19**, 129 (1980).
(4) W. C. Trogler, *Inorg. Chem.*, **19**, 697 (1980).
(5) G. J. Wessel and D. J. W. Ijdo, *Acta Crystallogr.*, **10**, 466 (1957).
(6) B. Briat, M. F. Russel, J. C. Rivoal, J. P. Chapelle, and O. Kahn, *Mol. Phys.*, **34**, 1545 (1977); L. Dubicki and Y. Tanabe, *ibid.*, **34**, 1531 (1977).
(7) I. W. Johnstone, K. J. Maxwell, and K. W. H. Stevens, *J. Phys. C*, **14**, 1297 (1981).
(8) O. Kahn and B. Briat, *Chem. Phys. Lett.*, **32**, 376 (1975).
(9) J. C. Beswick and D. E. Dugdale, *J. Phys. C*, **6**, 3326 (1973).
(10) J. D. Black, J. T. R. Dunsmuir, I. W. Forrest, and A. P. Lane, *Inorg. Chem.*, **14**, 1257 (1975).
(11) I. W. Johnstone, B. Briat, and D. J. Lockwood, *Solid State Commun.*, **35**, 689 (1980).
(12) P. M. Levy, *Phys. Rev.*, **177**, 509 (1969).
(13) M. E. Lines, *J. Chem. Phys.*, **55**, 2977 (1971).
(14) V. A. Sapozhnickov, A. E. Nikiforov, V. Ya. Mitrofanov, and A. N. Men, *Sov. Phys.—Solid State (Engl. Transl.)*, **16**, 2167 (1975); K. I. Kugev and D. I. Khomskii, *ibid.*, **17**, 235 (1975).
(15) N. Fuchikami and Y. Tanabe, *J. Phys. Soc. Jpn.*, **45**, 1559 (1978).
(16) M. V. Eremin, V. N. Kalinenkov, and Yu. V. Rakitin, *Phys. Status Solidi B*, **89**, 503 (1978).

0020-1669/81/1320-4193$01.25/0

polarization or temperature is still lacking. Magnetic susceptibility data are available for powders of $[Et_2NH_2]_3Ti_2Cl_9$[18,19] and for the corresponding cesium salt over the temperature range 80–300 K[20] and 4.2–70 K.[21]

Second, the $^2T_2$ (O_h) ground state of Ti^{3+} is, in principle, subjected to a Jahn–Teller effect, and this might have important consequences regarding exchange interactions.[22] In general, the large number of parameters to be included in the treatment of the $^2T_2 \times {}^2T_2$ coupling would probably preclude a deep insight into most physical data on titanium pairs. It turns out, however, that a simplification occurs for $Cs_3Ti_2Cl_9$ and that a phenomenological model provides an account for the gross features of our data.

The present study is devoted to a detailed spectroscopic and magnetic investigation of $Cs_3Ti_2Cl_9$ oriented single crystals. Although our main goal is the description and understanding of the ground-state manifold, we also report on a few other physical characteristics of our material.

Experimental Section

Preparation of $Cs_3Ti_2Cl_9$. This compound is reported to melt without decomposition at 705 °C.[23] Our starting materials were thoroughly dried ultrapure cesium chloride and anhydrous titanium trichloride (98%) supplied by Ventron. The latter was used in slight excess (8%) without being further purified. After being evacuated around 100 °C, the quartz ampule was sealed under vacuum and placed in a Bridgman furnace. Three series of materials were obtained under different experimental conditions. In two of them, the $CsCl–TiCl_3$ mixture was heated slowly while, in the third one, it was heated to the temperature of complete fusion rapidly so as to reduce the disproportionation of $TiCl_3$ to a minimum.[2] Large single crystals of good optical quality were obtained in the three instances, their optical properties being found identical. These crystals cleave easily, either perpendicular or parallel to the trigonal c axis. For absorption measurements, they were sealed on a silica window with glycol phthalate and then ground to the desired thickness (~40–50 μm) and polished on alumina. Our samples were protected from excessive humidity by storing them over magnesium perchlorate. An atomic spectroscopy analysis of several crystals indicated that they contain a substantial amount of residual iron ($Fe/Ti = (3–4) \times 10^{-3}$) but no chromium ($Cr/Ti \approx 10^{-6}$).

Spectroscopic Data. Absorption spectra were taken with a Cary 17 or a homemade[6] instrument with use of a cold finger (300–80 K) or a gas flow (105–8 K) cryostat. Magnetic circular dichroism (MCD) work was carried out under 0.7 T with an instrument described elsewhere.[24] Raman spectra were excited with the 5145-Å argon line (200 mW), the sample being mounted in a variable-temperature cryostat in the $X(\alpha\rho)Z$ conventional geometry (α and ρ stand for the polarization of the incident and the emergent beams, respectively) (Z along the unique axis). Infrared data were taken at 300 K on thin crystals, on a Perkin-Elmer 225 instrument (200–4000 cm^{-1}); EPR was investigated in the X band on a Varian spectrometer.

Magnetic Data. Magnetic measurements were performed with a Faraday-type magnetometer equipped with a He continuous-flow cryostat built by Oxford Instruments. We studied the temperature range 3.8–320 K, with a magnetic field of about 1.2 T. Mercury tetrakis(thiocyanato)cobaltate(II) was used as a susceptibility standard. The samples were single crystals of about 10 mg orientated with their c axis in an horizontal plane. The directions of the principal susceptibilities $\chi_\parallel$ and $\chi_\perp$ were determined at room temperature by rotating the electromagnet and looking for the extremes of the susceptibilities. The uncertainty on the temperature is less than 0.1 K and the uncertainty on the susceptibility is about 5×10^{-6} cm^3 mol^{-1}. All our measurements have been corrected for diamagnetism (-345×10^{-6} cm^3 mol^{-1}), as estimated from Pascal's tables.

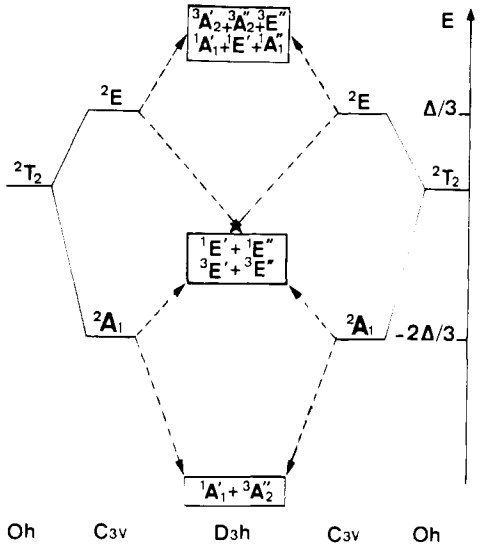

Figure 1. Schematic energy level diagram for the ground multiplet of $Cs_3Ti_2Cl_9$.

Theoretical Model

The $^2T_2$ ground term of each Ti^{3+} ion splits into $^2A_1$ at energy $-2\Delta/3$ and ^2E at $\Delta/3$ under the C_{3v} trigonal field. When spin–orbit coupling is ignored, exchange interaction between the two ions leads to the spectroscopic terms indicated in Figure 1 in a qualitative fashion, with notations appropriate for D_{3h} symmetry. One phenomenological Hamiltonian appropriate to describe this situation is shown by eq 1.[21] $\mathcal{H}_A$

$$\mathcal{H} = \mathcal{H}_A + \mathcal{H}_B + \mathcal{H}_{D_A} + \mathcal{H}_{D_B} + \mathcal{H}_{SS} + \mathcal{H}_{OO} + \mathcal{H}_{SO} \quad (1)$$

and $\mathcal{H}_B$ are the electronic Hamiltonians for each of the metallic centers noted A and B in pure octahedral ligand fields. The eigenfunctions of $\mathcal{H}_A$ (or $\mathcal{H}_B$) are the functions associated to the $^2T_2$ ground term. The two following terms describe the trigonal distortion around A and B. $\mathcal{H}_{D_A}$ (or $\mathcal{H}_{D_B}$) splits the $^2T_2$ term into $^2A_1$ and ^2E separated by Δ, taken as positive if the ground term is the orbital singlet. They have the classical form $\mathcal{H}_{D_{A(B)}} = (\Delta/3)(2 - Lz_{A(B)}^2)$.

$\mathcal{H}_{SS}$ is the spin–spin coupling operator, which removes the spin degeneracy of the eigenfunctions of $\mathcal{H}_A + \mathcal{H}_B$. A good description of the splittings between spin singlets and spin triplets is given by

$$\mathcal{H}_{SS} = -\hat{J}\hat{S}_A \cdot \hat{S}_B \quad (2)$$

where $\hat{J}$ is an orbital operator such as

$$\langle \Gamma,i|\hat{J}|\Gamma',j\rangle = J_\Gamma \delta_{\Gamma\Gamma'}\delta_{ij}$$

$|\Gamma,i\rangle$ is one of the eigenfunctions of $\mathcal{H}_A + \mathcal{H}_B$ transforming as one component of the Γ (=A_1, E, T_1, or T_2) irreducible representations contained in the direct product $T_2 \times T_2$. $\mathcal{H}_{OO}$ is an orbit–orbit coupling parameter removing partially the orbital degeneracy of the eigenfunctions of $\mathcal{H}_A + \mathcal{H}_B$. It takes the form $\mathcal{H}_{OO} = -\hat{K}\hat{L}_A \cdot \hat{L}_B$, where $\hat{K}$ is a spin operator such as

$$\langle S,M_S|\hat{K}|S',M_S'\rangle = K_{2S+1}\delta_{SS'}\delta_{M_SM_S'}$$

Finally, $\mathcal{H}_{SO}$ is the nonphenomenological spin–orbit coupling operator defined as

$$\mathcal{H}_{SO} = k\lambda(\hat{L}_A \cdot \hat{S}_A + \hat{L}_B \cdot \hat{S}_B)$$

where parameter for the $^2T_2$ ground term of the Ti^{3+} ion and k is an orbital reduction factor. Both λ and k are assumed to be isotropic hereafter.

(17) G. W. A. Fowles and B. J. Russ, *J. Chem. Soc. A*, 517 (1967).
(18) P. C. Crough, G. W. A. Fowles, and R. A. Walton, *J. Chem. Soc. A*, 972 (1967).
(19) C. R. Barraclough and A. K. Gregson, *J. Chem. Soc., Faraday Trans. 2*, 177 (1972).
(20) R. Saillant and R. A. D. Wentworth, *Inorg. Chem.*, **7**, 1606 (1968).
(21) O. Kahn, *Mol. Phys.*, **29**, 1039 (1975).
(22) See, e.g., B. S. Tsukerblat and B. G. Vekhter, *Sov. Phys.—Solid State (Engl. Transl.)*, **14**, 2204 (1973).
(23) D. V. Korol'kov and G. N. Kudryashova, *Russ. J. Inorg. Chem. (Engl. Transl.)*, **13**, 850 (1968).
(24) J. Badoz, M. Billardon, A. C. Boccara, and B. Briat, *Symp. Faraday Soc.*, **3**, 27 (1969).

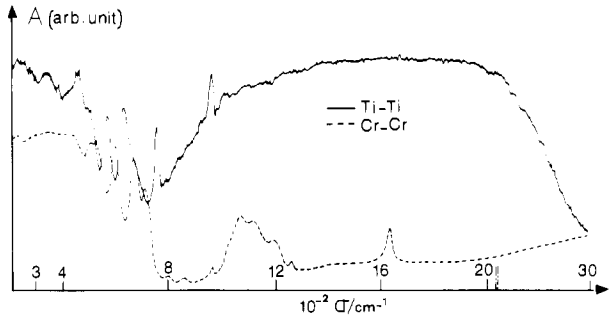

Figure 2. Infrared absorption spectra of $Cs_3Ti_2Cl_9$ (—) and $Cs_3Cr_2Cl_9$ (---).

The above Hamiltonian is diagonalized with use of the 9 spin-singlet and 27 spin-triplet functions built from the determinantal products $|\psi_{Ai}\psi_{Bj}|$ as a basis set. ψ_{Ai} and ψ_{Bj}, i and j varying from 1 to 6, are the t_{2g} functions appropriate for a d electron in an octahedral field with the axis of quantization taken as the threefold axis. In order to compute the principal magnetic susceptibilities, the parallel and perpendicular Zeeman perturbations are diagonalized with use of the eigenfunctions of $\mathcal{H}$ as a new basis set. The first- and second-order Zeeman coefficients are then calculated and introduced in the Van Vleck equations giving $\chi_\parallel$ and $\chi_\perp$ vs. T.

In the general case, all the parameters Δ, J_Γ, K_{2S+1}, λ, and k have an effect upon the magnetic properties of the pair. In the specific case of $Cs_3Ti_2Cl_9$, the situation is fortunately relatively simple. Indeed, we shall see that the different spectroscopic and magnetic studies allow us to assert that Δ is positive and large so that only the $^1A_1'$ and $^3A_2''$ levels arising from the interaction $^2A_1 \times {}^2A_1$ are thermally populated in the temperature range 3.8–300 K. It turns out that the thermic variations of $\chi_\parallel$ and $\chi_\perp$ will depend essentially on two parameters, namely, the trigonal distortion Δ and the energy gap J_{A_1} between the low lying states $^1A_1'$ and $^3A_2''$, that we shall note simply J in the following. The other J_Γ values as well as those of K_{2S+1}, λ, and k define the relative positions of the levels arising from $^2A_1 \times {}^2E$ and $^2E \times {}^2E$. These levels are located at energies around Δ and 2Δ, respectively, above the barycenter of the two lowest lying levels $^1A_1'$ and $^3A_2''$ (Figure 1), and their second-order effect on the magnetic properties will depend on Δ.

Until now, vibronic coupling has been ignored. We shall introduce it in the last section in order to explain some slight discrepancy between the predictions of the static model and the experiment.

Discussion of Spectroscopic Data

Infrared Absorption. Electronic transitions are electric dipole allowed among several sublevels in the ground manifold of $Ti_2Cl_9^{3-}$, via either the single ion or the exchange mechanism. It was especially interesting to investigate the spectral region at $\sigma > 400$ cm^{-1} since (i) electronic bands, if present, cannot be masked by vibrational features and (ii) $Cr_2Cl_9^{3-}$ has no electronic lines and can therefore serve as a reference material.

Indeed, our unpolarized spectra on crystals (Figure 2) indicate very clearly that electronic absorption occurs for titanium pairs in the 800–3000-cm^{-1} region. Although the signal presents a flat maximum because the absorbance is too high, one can make an estimate of the wavenumber $\bar{\sigma}$ corresponding to the barycenter of the band: $\bar{\sigma} \sim 1600$ cm^{-1}. This demonstrates that Δ in Figure 1 must have roughly this magnitude; i.e., the trigonal field is very large.

Weaker and sharper vibrational features in our spectra are due to traces of water (on surfaces), carbon dioxide, and probably oxides.

Raman Experiments. Electronic Raman bands usually appear significantly broader and weaker than vibrational lines.

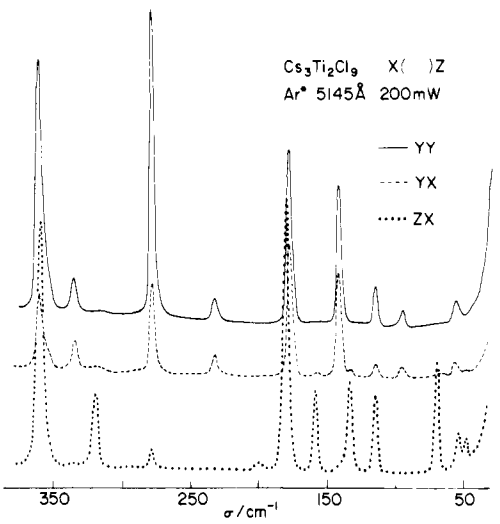

Figure 3. Polarized Raman spectra of $Cs_3Ti_2Cl_9$ around 8 K.

Table I. Observed Raman Frequencies (cm^{-1}) for $Cs_3Cr_2Cl_9$ and $Cs_3Ti_2Cl_9$ (Internal Modes of Vibration)

	$Cs_3Cr_2Cl_9$[a]	$Cs_3Ti_2Cl_9$[b]
4 A_{1g}	378	360
	283	278
	200	177
	138	144
5 E_{2g}	346	335
	237	232
	196	177
	161	140
	106	96
4 E_{1g}	337	319
	199	179
	172	158
	145	132

[a] From ref 10. [b] Present work.

Several of them being observed for $TiCl_3$ diluted into $CsMgCl_3$,[25] this was an encouragement to make a similar search in the case of $Cs_3Ti_2Cl_9$. Unfortunately, our measurements up to 1300 cm^{-1} have been unsuccessful in this respect. The most likely explanation for this failure is that we could not excite the bulk of our crystal with the argon line because of prohibitive absorption.

By contrast, the polarized vibrational spectra were obtained without any difficulty around 8 K (Figure 3). Actually, the scattering cross section is significantly larger than for the previously examined chromium derivative,[11] especially for the ZX spectrum. The frequencies of the 13 Raman-active internal modes of vibration are given in Table I for the sake of characterization. They appear very close to those observed for $Cs_3Cr_2Cl_9$ (Table I). Important polarization leakages are present in our spectra (Figure 3). This occurs because we excite the crystal in a preresonant region, especially when the laser beam is polarized along the c axis.

Visible and Near-UV Optical and Magnetooptical Data. Our polarized absorption spectra are shown in Figures 4–6, for the energy range 8000–33 000 cm^{-1}. The locations of the main peaks and shoulders are as indicated in Table II. The σ and axial (Figures 4 and 5) spectra are identical. Transitions are therefore electric dipole allowed, as expected for a D_{3h} site group symmetry. Furthermore, they are strongly polarized π or σ (Table II), this indicating a strong trigonal field. For convenience, we shall comment separately on our results for the near-infrared band and the visible–ultraviolet region.

(25) I. Johnstone and B. Briat, unpublished results.

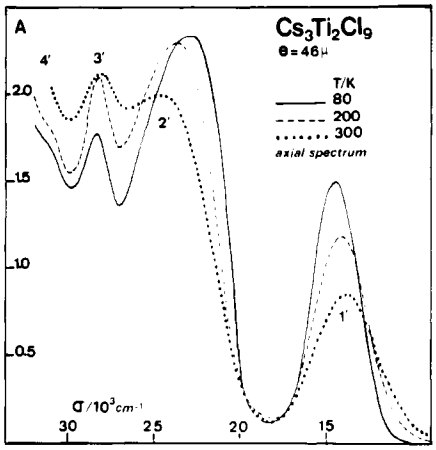

Figure 4. Axial absorption spectrum of $Cs_3Ti_2Cl_9$ at various temperatures.

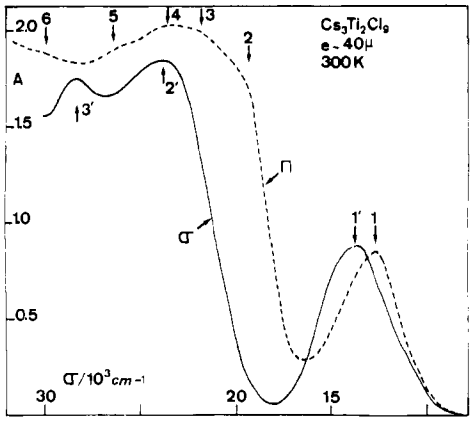

Figure 5. Polarized spectra (π and σ) of $Cs_3Ti_2Cl_9$ at 300 K (π and σ stand for the electric vectors of the beam parallel and perpendicular to the unique axis).

Table II. Energy (cm^{-1}) Corresponding to the Band Maxima and Shoulders of the Polarized Spectra of $Cs_3Ti_2Cl_9$ at 300 K (in Reference to Figure 5)

	π		σ
1	12 900	1'	14 200
2	19 800	2'	23 700
3	22 600	3'	28 500
4	24 200	4'	31 000
5	26 800		
6	29 500		

(a) Near-IR Band. Two important conclusions emerge from our measurements: (i) The axial (and σ) spectra show a very unusual increase in intensity when the temperature is lowered. A detailed study of this variation has been done at 12 temperatures; a few representative spectra are shown in Figure 4. By contrast, the intensity of the π spectrum (Figure 6) presents essentially no variation with temperature. (ii) None of our samples exhibit any measurable magnetic circular dichroism signal under 0.7 T in the whole temperature range 300–8 K. An upper limit of the difference of absorbance for left and right circular polarizations is estimated to be around $\Delta A = 10^{-4}$ at 14 500 cm^{-1}, the corresponding absorbance being roughly 1.

Considering all the literature on MCD spectroscopy,[26] such a low value for ΔA implies that the lowest substate in the ground manifold is diamagnetic, any paramagnetic term lying several hundreds of wavenumbers above it. This conclusion is reinforced by an analysis of the temperature variation of the axial spectrum in terms of the zeroth-order moment of the band: $M_0 = \int (A/\sigma)\, d\sigma$. Assuming a crude two-level model for the ground state, with degeneracy 1 and d respectively, we have attempted to fit our data with a law of the type $M_0 \approx (1 + de^{-x})^{-1}$, where $x = \delta/kT$ and δ is the splitting between the multiplet and the singlet. Considering plausible values for d and experimental errors due to the choice of the base line for each absorption curve, we stress the fact that the set $d = 3$, $\delta \approx 500 \pm 25$ cm^{-1} provides a satisfactory account for our data. This suggests that δ corresponds to the separation $|J|$ between the spin singlet and spin triplet arising from the exchange coupling of two $^2A_1$ states.

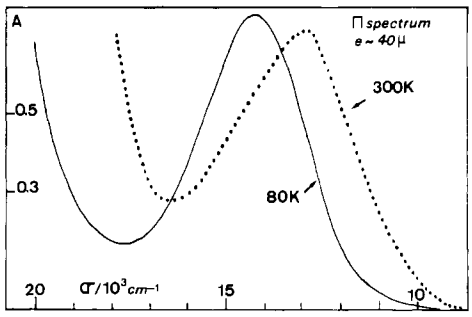

Figure 6. Temperature dependence of the π spectrum.

Considering that the spin–orbit coupling and the trigonal field have little influence on the ^2E_g octahedral state, it is quite reasonable to assume that the broadening of the absorption band is caused principally by coupling of the excited state of each $TiCl_6^{3-}$ unit with the tetragonal e mode. Then, by analogy with the $^5T_{2g} \rightarrow {}^5E_g$ situation encountered for Fe^{2+} in MgO,[27] the second-order moment of the absorption curve at 0 K leads to an estimate of the Jahn–Teller energy $E_{JT} \sim$ 5000–7000 cm^{-1}, depending upon the mean frequency, which is assumed for the active phonons. The coupling is therefore very strong, consistent with the fact that no zero phonon line is observed.

(b) Visible–Ultraviolet Regions. Our low-temperature polarized spectra present several bands between 20 000 and 33 000 cm^{-1} (Table II). The corresponding extinction coefficient is remarkably small ($\epsilon \approx 100$) as compared to that associated with the near-infrared d–d band ($\epsilon \sim 40$). This result, in itself, precludes an assignment to fully allowed charge-transfer transitions. Furthermore such transitions are expected at energies higher than 28 000 cm^{-1}, as observed for Ti^{3+} doped into AgCl.[28]

One of the high-energy bands (3' in Table II and Figure 4) becomes weaker when the crystal is cooled down. A similar observation has been made in a study of $TiCl_3$.[29] Such a behavior can possibly occur if we consider the simultaneous excitation of the two ions of the pair into the ^2E_g octahedral state via the exchange-induced dipole mechanism.

We are nevertheless left with several unexplained features. We believe that they are due to the occurrence of iron impurities in our crystals. This is supported by the fact that Fe^{3+} in Cs_2NaYCl_6 (O_h site symmetry) shows[30] absorption bands around 25 000, 28 000, and 32 000 cm^{-1}, i.e., at roughly the energies noted in Table II.

EPR Results. Our samples were also investigated with use of EPR at 9.08 GHz and variable temperature (5–60 K). For all orientations and a field up to 1 T, signals were only observed in the region $g \approx 1.52$–2.03, representative data being shown in Figure 7.[31]

(26) See, e.g., P. J. Stephens, *Adv. Chem. Phys.*, **35**, 197 (1976).

(27) A. Hjortsberg, B. Nygren, J. Vallin, and F. S. Ham, *Phys. Rev. Lett.*, **39**, 1233 (1977).
(28) W. Ulrici, *Phys. Status Solidi B*, **51**, 493 (1972).
(29) F. Cavallone, I. Pollini, and G. Spinolo, *Phys. Status Solidi B*, **45**, 405 (1971).
(30) H. Güdel and K. Neuenschwander, private communication.

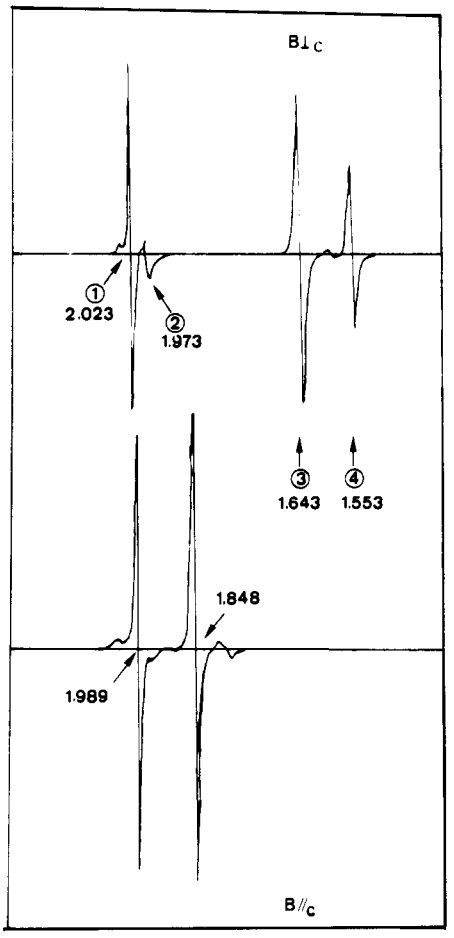

Figure 7. EPR spectra (9 GHz) for *B* parallel and perpendicular to the *c* axis (4.2 K).

In view of our magnetooptical and magnetic results (see subsequent sections), no line is actually due to titanium pairs. Our preliminary results are however worth being mentioned since they serve to characterize our material and point toward interesting future work. In this respect, we found that, upon varying T from 5 to 60 K, the intensity of lines 1 and 2 in Figure 7 reaches a maximum around 35 K. Furthermore, they show only a weak anisotropy. These features strongly suggest that we are dealing with transitions within the state of total spin $S = 1$ of Fe–Fe pairs. $Cs_3Ti_2Cl_9$ would therefore act as a diamagnetic host, which can be doped with paramagnetic trivalent ions. This possibility seems particularly promising in the case of iron since $Cs_3Fe_2Cl_9$ (grown from solution) can hardly be handled.[32]

Other features in the EPR spectra result from a complicated mixture of uncoupled Fe^{3+} or Ti^{3+}, Ti–Fe pairs, and possibly Ti^{2+}. They are consistent with the fact that the trigonal field for Ti^{3+} is important (with the orbital singlet lowest) since, otherwise, some g factors would depart much more markedly from 2, as for Ti^{3+} in Al_2O_3 ($g_\parallel = 1.067$).

Discussion of Magnetic Data

Our spectroscopic measurements have led to an understanding of the gross features in the ground-state manifold. It turns out however that the most decisive information concerning the nature of the low lying states has arisen from our magnetic measurements.

We studied the magnetic properties of four different crystals. For all of them, the parallel susceptibility $\chi_\parallel$ is weaker than the perpendicular one $\chi_\perp$. The magnetic anisotropy defined as $\Delta\chi = \chi_\perp - \chi_\parallel$ increases very smoothly when the crystals cool down from 320 to 100 K and then remains constant below 100 K. $\Delta\chi$ is equal to 410×10^{-6} cm^3 mol^{-1} at 320 K and to 540×10^{-6} cm^3 mol^{-1} at 100 K. Both $\chi_\parallel$ and $\chi_\perp$ decrease when the crystals cool down, reach a broad minimum for a temperature depending on the sample, located between 100 and 140 K, and then increase again below this temperature. This behavior corresponds to that which has been observed by several authors for polycrystalline samples. The better the quality of the crystal appears when examined under a microscope, the lower the temperature for which $\chi_\parallel$ and $\chi_\perp$ are minimum.

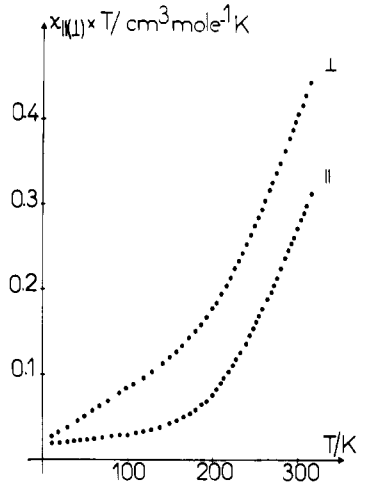

Figure 8. Temperature dependence of χT for one of the $Cs_3Ti_2Cl_9$ samples.

The increase of $\chi_\parallel$ and $\chi_\perp$ at very low temperature is due to a paramagnetic impurity, which acts as a strong perturber since the measured susceptibilities are weak owing to the magnitude of the antiferromagnetic coupling between the Ti(III) ions in the $Ti_2Cl_9^{3-}$ pair. An unambiguous proof of the extrinsic origin of the increase of $\chi_\parallel$ and $\chi_\perp$ at low temperatures can be given as will be indicated now. Figure 8 shows the temperature dependence of $\chi_\parallel T$ and $\chi_\perp T$ for one of the samples. As expected for a pair of antiferromagnetically coupled ions, both $\chi_\parallel T$ and $\chi_\perp T$ decrease when the crystals cool down. Below 100 K, the magnetic data very closely follow linear laws:

$$\chi_\parallel T/\text{cm}^3\ \text{mol}^{-1}\ \text{K} = 0.0189 + 125 \times 10^{-6} T/\text{K}$$

$$\chi_\perp T/\text{cm}^3\ \text{mol}^{-1}\ \text{K} = 0.0189 + 665 \times 10^{-6} T/\text{K}$$

The borderline value $\chi_\parallel T = \chi_\perp T = 0.0189$ cm^3 mol^{-1} K $= \chi^1 T$ when T approaches zero corresponds to the paramagnetism of the impurity, which appears therefore isotropic. This behavior is consistent with the presence in our material of unpaired Fe^{3+} or Ti^{3+}, but it implies that the latter, if present, is in a reasonably pure singlet orbital state. Magnetic susceptibility and EPR data are therefore fully consistent.

Assuming a Curie law for χ^1 over the whole temperature range then irrespective of the actual nature of the impurity (relative concentration ρ), it is possible to correct the measured susceptibility χ and obtain that of the dimer from the formula

$$\chi^D T(1 - \rho) = \chi T - 0.0189\ \text{cm}^3\ \text{mol}^{-1}\ \text{K}$$

ρ, which is in any case very weak, can be safely disregarded since it will only lead to a very slight change of scale for χ^D. From the data in Figure 8, we have derived the temperature dependence of $\chi^D{}_\parallel$ and $\chi^D{}_\perp$ as shown in Figure 9. Results identical to within $\pm 20 \times 10^{-6}$ cm^3 mol^{-1} were obtained when similarly treating our data for the other samples. It is thus firmly established that Figure 9 represents the actual magnetic behavior of $Cs_3Ti_2Cl_9$ with a very good accuracy.

(31) K. Robinson and B. Briat, unpublished results.
(32) H. Güdel, private communication.

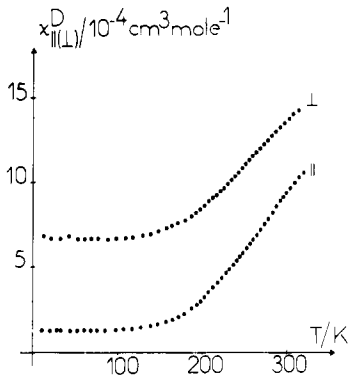

Figure 9. Temperature dependence of the corrected susceptibility χ^D ($\parallel$ and $\perp$) for the titanium dimer.

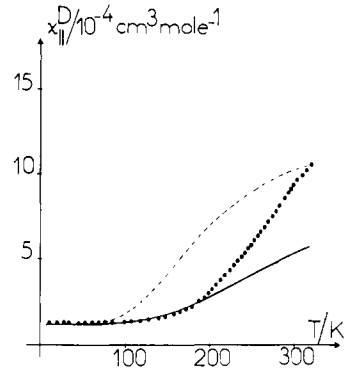

Figure 10. Comparison of the experimental (···) and computed [(- - -) $J = -440$ cm^{-1}; (—) $J = -630$ cm^{-1}] data for $\chi^D_{\parallel}$.

This figure indicates clearly that the ground level for the Ti–Ti pair is nonmagnetic, i.e., is a spin singlet and an orbital singlet, and that this state is separated by several hundred wavenumbers from the first magnetic level. The question that is stated now is whether this level is $^1A_1'$ arising from $^2A_1 \times {}^2A_1$, or $^1A_1'$ (or $^1A_1''$) arising from $^2E \times {}^2E$, in other words, whether the single-ion ground term of Ti(III) is $^2A_1$ or ^2E. A clear answer may be obtained by simulating theoretically the magnetic behavior of $Cs_3Ti_2Cl_9$ by means of the Hamiltonian given in eq 1 (static model). Actually, *the only way to obtain a magnetic anisotropy* $\Delta\chi^D$ that is *positive and smoothly increasing when the temperature cools down is to impose a positive trigonal distortion* Δ (^2E highest). In a qualitative way, the magnetic properties of $Cs_3Ti_2Cl_9$ represented in Figure 9 prove without any ambiguity that the two low lying levels in $Ti_2Cl_9^{3-}$ are $^1A_1'$ and $^3A_2''$, the latter being separated by several hundred wavenumbers from the ground level, and that these levels arise from the interaction between the two single-ion ground terms $^2A_1$. This result invalidates the conclusions drawn[33] from the study of the magnetic properties of powdered samples.

We can now attempt a quantitative treatment of the electronic structure of $Ti_2Cl_9^{3-}$ to determine the J energy gap between the $^1A_1'$ and $^3A_2''$ low lying levels and the Δ trigonal distortion. At first view, the determination of J might appear easy. Indeed, in the absence of spin–orbit coupling, all the second-order Zeeman coefficients, which occur in the expression of the parallel susceptibility $\chi^D_{\parallel}$, would be identically zero since the $^1A_1'$ and $^3A_2''$ low lying levels do not couple through the parallel orbital component $\beta k L_{\parallel} H_{\parallel}$ of the Zeeman operator with any other pair levels arising from the $^2T_{2g} \times {}^2T_{2g}$ exchange interaction. It turns out that $\chi^D_{\parallel}$ would exactly follow the equation giving the temperature dependence of the susceptibility for a pair of spin doublets without a first-order orbital angular momentum:[34]

$$\chi^D_{\parallel} = \frac{2N\beta^2g^2}{kT}\left[3 + \exp\left(-\frac{J}{kT}\right)\right]^{-1} + N\alpha \qquad (3)$$

If one takes into account spin-orbit coupling, the second-order Zeeman coefficients are no longer all identically zero; nevertheless, taking the value $\lambda = 150$ cm^{-1} of the free ion for the spin–orbit coupling parameter and giving values compatible with the experimental data to J and Δ, we checked that the variation of $\chi^D_{\parallel}$ vs. T, to which the exchange Hamiltonian (eq 1) leads, very weakly deviates from eq 3. Consequently, the fitting of the experimental values of $\chi^D_{\parallel}$ with this equation should lead to a relatively accurate determination of J. In fact, this is not the case; taking $N\alpha = 125 \times 10^{-6}$ cm^3 mol^{-1} (value of $\chi^D_{\parallel}$ below 100 K), one does not find any J,g set compatible with experimental data. Whatever the value of g (around 2.00) may be, the energy gap J between $^1A_1'$ and $^3A_2''$ appears to enhance significantly when the temperature decreases. For instance, in Figure 10, we compared the theoretical curves deduced from eq 3 for $g = 2.00$, $J = -440$ cm^{-1} and $g = 2.00$, $J = -630$ cm^{-1} with the experimental data of Figure 9. It is clear that the concavity of the theoretical curves is different from that of the experimental one. Whereas $J = -440$ cm^{-1} appears to be the value for the $^1A_1'$–$^3A_2''$ energy gap at 320 K, $J = -630$ cm^{-1} fits the experimental data around 120 K. Owing to the accuracy of the measurements carried out, we may assert that the above disagreement is not due to an experimental uncertainty, but rather reflects the actual behavior of the compound. In the next section, we shall propose an interpretation of this behavior.

If one takes now for J an average value $J = -525$ cm^{-1}, one can obtain an estimate of the trigonal distortion parameter Δ and of the orbital reduction factor k by comparing the experimental anisotropy $\Delta\chi$ to the anisotropy calculated with use of the Hamiltonian (1). The best fit is obtained for $\Delta = 1400$ cm^{-1} and $k = 0.85$. These two parameters being, as expected, strongly correlated, the uncertainty on their values is rather important. The uncertainty on Δ can be estimated to ± 200 cm^{-1} and that on k to ± 0.1.

Even if an accurate value of J cannot be deduced from the temperature dependences of the magnetic susceptibilities, it is nevertheless quite clear that the coupling between the Ti(III) ions is very strongly antiferromagnetic. In this respect, one can notice that the situation is very different in $Cs_3Cr_2Cl_9$ where J is equal to -13 cm^{-1}.[8]

In order to compare the exchange parameter in the two compounds, it is useful to decompose J in eq 2 into orbital contributions according to[35]

$$J = \frac{1}{n^2}\sum_{ij} J_{ij} \qquad (4)$$

where n is the number of unpaired electrons per metallic center and J_{ij} is the exchange integral $\langle\phi_{Ai}(1)\phi_{Bj}(2)|\mathcal{H}'|\phi_{Ai}(2)\phi_{Bj}(1)\rangle$. The ϕ_{Ai} and ϕ_{Bi} are the magnetic orbitals around the A and B centers, respectively, and $\mathcal{H}'$ is the electrostatic-exchange Hamiltonian. If we note ϕ_{Ai} ($i = 1$–3) the magnetic orbitals centered on A transforming as the irreducible representations $A_1(\phi_{A1})$ and $E(\phi_{A2}, \phi_{A3})$ of the C_{3v} site group, we can express the exchange parameters J_{TiTi} of $Cs_3Ti_2Cl_9$ and J_{CrCr} of $Cs_3Cr_2Cl_9$ as

$$J_{TiTi} = J_{11} \approx -525 \text{ cm}^{-1}$$

$$J_{CrCr} = \tfrac{1}{9}(J_{11} + 2J_{22} + 4J_{12} + 2J_{23}) = -13 \text{ cm}^{-1}$$

(33) O. Kahn, *Mol. Phys.*, **31**, 957 (1976).
(34) B. Bleaney and K. D. Bowers, *Proc. R. Soc. London, Ser. A*, **214**, 451 (1952).
(35) J. H. Van Vleck, *Phys. Rev.*, **45**, 405 (1934).

The orbitals ϕ_{A1} and ϕ_{B1} point toward each other, so that J_{11} is the most negative contribution in the expression of J_{CrCr}. The relative orientations of the magnetic orbitals of E symmetry are such that J_{22} should be very weakly negative. As for the J_{12} and J_{23} contributions, they are positive since the involved magnetic orbitals are orthogonal. The difference in the magnitudes of J_{TiTi} and J_{CrCr} may be explained in two ways: (i) The J_{11} contribution in the chromium compound could be weaker in absolute value than 525 cm^{-1}. This would require a metal–metal separation in $Cs_3Ti_2Cl_9$ significantly shorter than in $Cs_3Cr_2Cl_9$. In spite of the quality of our crystals, all our attempts to determine their structure by X-ray diffraction were unsuccessful because of their fragility with respect to the X-ray beam. However we can notice that the two compounds are isomorphous and that their lattice parameters are very similar.[15] (ii) The J_{12} and J_{23} contributions could be strongly positive and nearly compensate the negative contributions J_{11} and J_{22}. This explanation, which does not require any dramatic modification of the geometry of the bridging network MCl_3M between $Cs_3Ti_2Cl_9$ and $Cs_3Cr_2Cl_9$, seems to us to be the most likely. Indeed several recent studies emphasized the importance of the ferromagnetic contributions in the exchange interaction.[36-38]

Role of Vibronic Coupling

We wish here to understand why the temperature dependence of $\chi^D_{\parallel}$ in $Cs_3Ti_2Cl_9$ is not described in a satisfying manner by eq 3 although, the spin–orbit coupling being very weak compared to the trigonal distortion, the second-order Zeeman coefficients in $\chi^D_{\parallel}$ are nearly negligible. In a more general way, we wonder why the exchange Hamiltonian (1) in which the nuclei are assumed to be at rest in their equilibrium positions does not lead to a good quantitative simulation of the magnetic properties of our compound.

The above situation contrasts with that which we have encountered so far[38-41] for a number of copper(II) dimers exhibiting a very strong antiferromagnetic interaction. In these complexes, the first single-ion excited level is located at about 10 000 cm^{-1} above the ground single-ion level.[42] By comparison, in $Ti_2Cl_9^{3-}$, the ^2E single-ion term lies much closer ($\sim$1400 cm^{-1}) to the ground term $^2A_1$. We believe therefore that the trigonal distortion might not be large enough to quench completely the effect of the vibronic coupling in the $^2T_2$ ground state of each Ti^{3+} ion.

In order to get a qualitative feeling about the influence of vibronic coupling on exchange interaction, we shall make the crude assumption that $^2T_2$ is only coupled to the Q_2 and Q_3 modes of symmetry e (in O_h symmetry) and frequency $\hbar\omega$.

The vibronic Hamiltonian for each $TiCl_6$ entity may be written as shown in eq 5. $\mathcal{H}_E$ is the electronic Hamiltonian

$$\mathcal{H} = \mathcal{H}^\circ_E + \mathcal{H}_N + \sum_{k=2,3}\left(\frac{\delta\mathcal{H}_E}{\delta Q_k}\right)_0 Q_k \qquad (5)$$

depending parametrically on the 15 modes of vibrations, $\mathcal{H}^\circ_E$ is the electronic Hamiltonian for the configuration of C_{3v} symmetry,[44] and $\mathcal{H}_N$ is the nuclear Hamiltonian. Let us call ϕ_i (i = 1–3) the eigenfunctions of $\mathcal{H}^\circ_E$ transforming as $A_1(\phi_1)$ and $E(\phi_2$ and $\phi_3)$, respectively. From the Wigner–Eckart theorem, the matrix elements of the vibronic coupling term in (5), with use of the ϕ_i's as a basis set, may be expressed[45-47] as eq 6, where K is the vibronic coupling parameter and the

$$\sum_{k=2,3}\left\langle \phi_i\left|\frac{\partial\mathcal{H}_E}{\partial Q_k}\right|\phi_j\right\rangle Q_k = k\sum_{k=2,3} h_k(i,j)Q_k \qquad (6)$$

matrices h_k are shown by eq 7.

$$h_2 = \begin{pmatrix} 0 & -2^{1/2}/2 & 0 \\ -2^{1/2}/2 & -1/2 & 0 \\ 0 & 0 & 1/2 \end{pmatrix}$$
$$h_3 = \begin{pmatrix} 0 & 0 & -2^{1/2}/2 \\ 0 & 0 & 1/2 \\ -2^{1/2}/2 & 1/2 & 0 \end{pmatrix} \qquad (7)$$

We denote $\varphi^{m,n}$ as the eigenfunctions of $\mathcal{H}_N$ in the harmonic approximation; m and n are the vibrational quantum numbers associated with the modes Q_2 and Q_3, respectively. Considering the vibronic coupling term as a perturbation, it is straightforward to derive the basis functions $\psi_1^{(1)m,n}$ on which the symmetry-adapted first-order vibronic functions associated with $^2A_1$ can be constructed. One finds eq 8 and 9, where μ

$$\psi_1^{(1)m,n} = \left[1 + \frac{2x}{\rho^2}(m+n+1)\right]^{-1/2}\left\{\phi_1\varphi^{m,n} - x^{1/2}\left[\frac{(m+1)^{1/2}\phi_2\varphi^{m+1,n} + (n+1)^{1/2}\phi_3\varphi^{m,n}}{\rho+1} + \frac{m^{1/2}\phi_2\varphi^{m-1,n} + n^{1/2}\phi_3\varphi^{m,n-1}}{\rho-1}\right]\right\} \qquad (8)$$

$$x = \frac{K^2}{4\hbar\mu\omega^3} \qquad (9)$$

is the reduced mass associated to the vibration and $\rho = \Delta/\hbar\omega$.

The corresponding energy at the second order is given by eq 10, E_0 being the eigenvalue of lowest energy of $\mathcal{H}_E^0$.

$$E^{m,n} = E_0 + \sum_k \hbar\omega_k(m_k + 1/2) - x\hbar\omega\left(\frac{m+n+2}{\rho+1} + \frac{m+n}{\rho-1}\right) \qquad (10)$$

Thus the vibronic coupling mixes the electronic functions ϕ_i. More precisely, the higher m and n are, the more important the contributions of ϕ_2 and ϕ_3 of symmetry E in the expression of the vibronic function associated to the ground level $^2A_1$. Actually, a qualitatively similar conclusion has been reached recently in a more general treatment where, in C_{3v} symmetry, both the doublet and the singlet issued from an octahedral T state are linearly coupled to a vibrational doublet.[48]

Let us consider now the exchange interaction $^2A_1 \times {}^2A_1$ between the two vibronic functions $\psi_{A1}^{(1)m,n}$ and $\psi_{B1}^{(1)m',n'}$ associated with the $TiCl_6$ units. From a qualitative point of view, one easily perceives that the interaction between the electronic functions ϕ_{A1} and ϕ_{B1}, which point toward each other, is much stronger than the interactions between ϕ_{A2} and ϕ_{B2} or ϕ_{A3} and ϕ_{B3} or between two orthogonal functions such as ϕ_{A1} and $\phi_{B2(3)}$. A semiquantitative justification of this has been given elsewhere.[49] Consequently, the more excited the

(36) O. Kahn, J. Galy and P. Tola, *J. Am. Chem. Soc.*, **100**, 3931 (1978).
(37) O. Kahn and M. F. Charlot, *Nouv. J. Chim.*, **4**, 567 (1980).
(38) J. P. Malrieu, private communication.
(39) J. J. Girerd, S. Jeannin, Y. Jeannin, and O. Kahn, *Inorg. Chem.*, **17**, 3034 (1978).
(40) M. F. Charlot, S. Jeannin, Y. Jeannin, O. Kahn, J. Lucrece-Abaul, and J. Martin-Frere, *Inorg. Chem.*, **18**, 1675 (1979).
(41) J. Galy, J. Jaud, O. Kahn, and P. Tola, *Inorg. Chim. Acta*, **36**, 229 (1979).
(42) C. Chauvel, J. J. Girerd, Y. Jeannin, O. Kahn, and G. Lavigne, *Inorg. Chem.*, **18**, 3015 (1979).
(43) J. Ferguson, *Prog. Inorg. Chem.*, **12**, 159 (1970).
(44) O. Kahn and S. Kettle, *Mol. Phys.*, **29**, 1039 (1975).
(45) W. Moffitt and W. Thorson, *Phys. Rev.*, **108**, 1251 (1957).
(46) F. S. Ham, *Phys. Rev. A*, **136**, 1727 (1965).
(47) M. D. Sturge, *Solid State Phys.*, **20**, 91 (1967).
(48) R. Lacroix, J. Weber, and E. Duval, *J. Phys. C*, **12**, 2065 (1979).
(49) O. Kahn, B. Briat, and J. Galy, *J. Chem. Soc., Dalton Trans.*, 1453 (1977).

vibronic levels deriving from $^2A_1$ are, the weaker the interaction between $\psi_{A1}^{(1)m,n}$ and $\psi_{B1}^{(1)m',n'}$. Hence, the singlet–triplet energy gap will depend on the vibronic levels under consideration. The more excited these vibronic levels are, the weaker this energy gap.

A more quantitative approach consists of calculating explictly the $J_{11}^{m,n,m',n'}$ energy gap between the spin triplet and the spin singlet arising from the interaction between the two vibronic levels associated with the $^2A_1$ single-ion ground terms and characterized by the quantum numbers m, n and m', n', respectively. $J_{11}^{m,n,m',n'}$ is defined as shown in eq 11.

$$J_{11}^{m,n,m',n'} = \langle\psi_{A1}^{(1)m,n}(1)\psi_{B1}^{(1)m',n'}(2)|\mathcal{H}'|\psi_{A1}^{(1)m,n}(2)\psi_{B1}^{(1)m',n'}(1)\rangle \quad (11)$$

From (8), (11) becomes (12), with the J_{ij}'s defined as in

$$J_{11}^{m,n,m',n'} = N[J_{11} + a_{12}J_{12} + a_{22}J_{22} + a_{23}J_{23}] \quad (12)$$

(2) and the N, a_{12}, a_{22}, and a_{23} coefficients given by eq 13–16.

$$N = \left[1 + \frac{2x}{\rho}(m + n + 1)\right]^{-1}\left[1 + \frac{2x}{\rho}(m' + n' + 1)\right]^{-1} \quad (13)$$

$$a_{12} = x\left[\frac{m + n + m' + n' + 4}{(\rho + 1)^2} + \frac{m + n + m' + n'}{(\rho - 1)^2}\right] \quad (14)$$

$$a_{22} = x^2\left[\frac{(m + 1)(m' + 1) + (n + 1)(n' + 1)}{(\rho + 1)^4} + \frac{(m + 1)m' + (n + 1)n' + m(m' + 1) + n(n' + 1)}{(\rho + 1)^2(\rho - 1)^2} + \frac{mm' + nn'}{(\rho - 1)^4}\right] \quad (15)$$

$$a_{23} = x^2\left[\frac{(m + 1)(n' + 1) + (n + 1)(m' + 1)}{(\rho + 1)^4} + \frac{(m + 1)n' + (n + 1)m' + m(n' + 1) + n(m' + 1)}{(\rho + 1)^2(\rho - 1)^2} + \frac{mn' + nm'}{(\rho - 1)^4}\right] \quad (16)$$

We have seen that J_{11} is much more negative than J_{22}. As for J_{12} and J_{23}, they are positive. It turns out that the more excited the vibronic levels are, the less negative $J_{11}^{m,n,m',n'}$. From the point of view of the magnetic properties, this leads to an apparent increase of $|J|$ in (2) when the temperature decreases.

In this model, the temperature dependence for the parallel magnetic susceptibility $\chi_\parallel$ may be easily obtained if we neglect the very small second-order Zeeman coefficients due to the spin–orbit coupling (see above); the energies of the spin singlet and of the spin triplet arising from the interaction between the vibronic levels m, n and m', n' may be expressed simply as in eq 17 and 18. $\chi_\parallel$ is then given by eq 19, where Y is defined as in eq 20.

$$E^{m,n,m',n'} = E^{m,n} + E^{m',n'} + (3J_{11}^{m,n,m',n'}/4) \quad (17)$$

$$E^{m,n,m',n'} = E^{m,n} + E^{m',n'} - (J_{11}^{m,n,m',n'}/4) \quad (18)$$

$$\chi_\parallel = \frac{2N\beta^2g^2}{kT}(3 + Y)^{-1} + N\alpha \quad (19)$$

$$Y = \frac{\sum_{m,n,m',n'} \exp\left(-\frac{E^{m,n} + E^{m',n'}}{kT}\right)}{\sum_{m,n,m',n'} \exp\left(\frac{J_{11}^{m,n,m',n'}}{kT}\right)\exp\left(-\frac{E^{m,n} + E^{m',n'}}{kT}\right)} \quad (20)$$

Taking $\Delta = 1400$ cm^{-1} and $\hbar\omega = 278$ cm^{-1},[18] we checked that the thermal variation of $\chi_\parallel$ can be reproduced fairly well within the frame of this vibronic scheme. Of course, several sets of parameters J_{ij} and x lead to a similar temperature dependence. It should be stressed however that a good fit can be obtained for $x \ll \rho^2$; i.e., our perturbation treatment appears to be quite reasonable a posteriori.

Conclusion

$Cs_3Ti_2Cl_9$ is a model material for the study of the exchange interaction between orbitally degenerate ions. This explains why several attempts have already been made to find out the nature and the relative energies of the low lying levels. Until now, such studies have been largely unsuccessful, essentially because they were carried out on polycrystalline samples.

Using the crystal-growing techniques of solid-state chemistry, we were able to obtain single crystals for both spectroscopic and magnetic studies. In order to describe properly the ground-state manifold of Ti–Ti pairs, we accumulated a large body of experimental data in a wide temperature range.

The two important questions which were stated were the following: (i) What are the sign and the magnitude of the trigonal distortion around each Ti(III) ion? (ii) What are the nature and the magnitude of the interaction that occurs between the two single-ion terms in the Ti–Ti pair?

Infrared spectroscopy and magnetic anisotropy measurements gave an unambiguous answer to the first question. For each $TiCl_6$ unit, the trigonal field is large, with $^2A_1$ lying about 1500 cm^{-1} below ^2E. Magnetic measurements provided the answer to the second question. The Ti(III) ions are very strongly antiferromagnetically coupled with a separation of roughly 525 cm^{-1} between the two low-lying levels $^3A_2''$ and $^1A_1'$ arising from the interaction $^2A_1 \times {}^2A_1$. A similar conclusion was also reached from our magnetic circular dichroism and polarized absorption data.

The above values characterizing the trigonal distortion and the exchange interaction, respectively, were derived on the basis of a static model, which we believe is essentially correct. In view however of a slight but significant discrepancy between our susceptibility data and the model predictions, we searched for an improvement of the theory. We suggest that vibronic coupling is the cause of the observed increase of the $^3A_2''$–$^1A_1'$ energy gap when the crystal is cooled down from room to very low temperatures.

Acknowledgment. Raman and EPR spectra were taken by I. Johnstone and K. Robinson while B.B. was a guest of Dr. J. Ferguson at the Australian National University. It is a pleasure to acknowledge here their contribution. We thank also M. Le Postellec for help in obtaining the infrared data and M. Nerozzi for growing the single crystals used in this study.

Note Added in Proof. We are grateful to one of the reviewers (G. L. McPherson), who kindly informed us of his unpublished determination of the structure of $Cs_3Ti_2Cl_9$. If Cl_1 and Cl_2 stand for the bridging and terminal ligands, respectively, the structural parameters are as follows: Ti–Cl_1 = 2.503 Å, Ti–Cl_2 = 2.328 Å, Ti–Ti = 3.191 Å, Cl_1TiCl_1 = 83.7°, Cl_2TiCl_2 = 95.2°. As anticipated in our discussion, this structure of $Ti_2Cl_9^{3-}$ is nearly identical with that of $Cr_2Cl_9^{3-}$ in $Cs_3Cr_2Cl_9$.

Registry No. $Cs_3Ti_2Cl_9$, 12052-06-1; $Cs_3Cr_2Cl_9$, 21007-54-5.